



Stability of a stratified shear flow, a model of fluid mud

Alice HARANG^{1,2}, **Olivier THUAL**^{1,2},
Pierre BRANCHER^{1,2}, **Thomas BONOMETTI**^{1,2}

1. Université de Toulouse, INPT, UPS, IMFT, Allée Camille Soula,
F-31400 Toulouse, France.

2. CNRS, IMFT, F-31400 Toulouse, France.

harang@imft.fr ; thual@imft.fr ; brancher@imft.fr ; thomas.bonometti@imft.fr

Abstract:

To improve the understanding of mud suspension in estuaries, a parametric stability analysis of a two-dimensional shear flow was carried out with a model of two miscible fluid layers of different mass density and dynamic viscosity. The direct numerical simulation code JADIM of IMFT (Institut de Mécanique des Fluides de Toulouse) is used to compute the temporal evolution of these flows. This study is completed by a linear stability study realized with the code LiSa developed at IMFT. A critical Richardson number close to 0.25 is observed. Results show that the characteristics of the most unstable modal wave number and the location of the interface instability, depend on the ratio of two fluid viscosity values. The model is initialized with continuous erf(z) vertical profiles for all quantities. Likely outcomes of this stability study are new parameterizations for realistic modelling of estuaries.

Received 12 November 2010, accepted 7 December 2010, available online 22 December 2010.

Translated version not certified, published under the responsibility of the article authors.

How to cite the original paper:

HARANG A., THUAL O., BRANCHER P., BONOMETTI T. (2010). *Stabilité d'un écoulement cisailé modélisant la crème de vase*. *Revue Paralia*, Vol. 3, pp 8.1-8.12.

DOI:10.5150/revue-paralia.2010.008 (disponible en ligne – <http://www.paralia.fr> – available online)

1. Introduction

Numerical models of estuaries, such as TELEMAC_3D or SIAM-3D for example, are used to deal with pollution or coastal settlement. Concerning erosion at the bottom of the estuary, these models are often based on the parameterization proposed by PARTHENIADE (1963) or PARCHURE & METHA (1985). However, these models can be improved by a more specific study of the interface between mud flow and water as proposed by LE NORMAND (1995) after coding TELEMAC_3D. In this way, we present a bi-dimensional study of the stability of the interface. Stability and mixing of stratified shear flow have been studied by CAULFIELD & PELTIER (2000). ERN *et al.* (2003) concentrate on shear flows with strongly stratified viscosity. KRANENBURG & WINTERWERP (1997) present a model validated by experiments, computing mud flow erosion by turbulence produced by wind or convected from other locations in the flow. As observations of the mud flow show its high viscosity, a highly viscous and very dense Newtonian fluid has been chosen to model mud flow. As explained in PHAM VAN BANG *et al.* (2007), mud flows are very complex to model because of the effect of time, forcing, thixotropy. For the present study, we have chosen a Newtonian fluid model with strong density and viscosity variations to get a first understanding of the response of the system to complex rheology. According to the model of mud flow vertical distribution proposed by MEHTA *et al.* (1989), the thickness of the shear profile can be much bigger than the density profile, and according to HOGG and IVEY (2003), Holmboe instabilities can develop at the interface between water and mud flows. However, we choose here the same thickness for the shear, density and viscosity profiles, in order to focus on the study of Kelvin-Helmoltz instabilities.

2. Model of mud flow

2.1 Model equations

Our study is based on the following equations:

$$\nabla \cdot \underline{u} = 0, \quad \frac{d\underline{u}}{dt} = -\frac{1}{\rho} \nabla P + \underline{g} + \frac{1}{\rho} \nabla \left[\mu \left(\nabla \underline{u} + {}^t \nabla \underline{u} \right) \right] \quad (1.a)$$

$$\frac{\partial \Phi}{\partial t} + \nabla \cdot (\Phi \underline{u}) = 0, \quad (1.b)$$

$$\rho = \rho_0(1 - \Phi) + \rho_1 \Phi, \quad \mu = \mu_0(1 - \Phi) + \mu_1 \Phi \quad (1.c)$$

which link incompressible Navier-Stokes equations (1.a), where \underline{g} is the acceleration of gravity, to the transport equation (1.b) of a volume fraction Φ which controls, through relations (1.c), the kinematic mixing of fluid particles of non-homogeneous density ρ and dynamic viscosity μ . Molecular diffusion of sediments is neglected here (see DEARDORFF & WILLIS, 1982)

The mixing of the two following fluids is considered: water, of density $\rho_0=1000 \text{ kg m}^{-3}$ and dynamic viscosity $\mu_0=10^{-3} \text{ Pa s}$, and the mud flow, of density $\rho_1=1360 \text{ kg m}^{-3}$ (MEHTA *et al.* 1989) and dynamic viscosity $\mu_1=1 \text{ Pa s}$. Both entities are then mixed and followed through the volume fraction of mud flow in the fluid, Φ . So, in these simulations, density and viscosity are linear functions of the volume fraction and then vary in the same way.

2.2 Base flow

To model vertical profiles of the concerned quantity near the water-mud flow interface, we consider the group of functions $F(\lambda, Z)$ defined by:

$$F(\lambda, Z) = \begin{cases} \lambda \left[1 + \operatorname{erf}\left(\frac{Z}{\lambda}\right) \right] & \text{if } Z \leq 0, \\ 1 - (1 - \lambda) \left[1 - \operatorname{erf}\left(\frac{Z}{1 - \lambda}\right) \right] & \text{if } Z \geq 0, \end{cases} \quad (2)$$

where Z is the non-dimensional vertical coordinate to be specified later, the origin of which being located at the interface the parameter λ controls the asymmetry of the fields located on both sides of the inflexion point, with continuity of the profile and its derivative around this point. The characteristics of this group of functions are described on figure 1. The function $\operatorname{erf}(z)$ is chosen as base function, in an empirical way, to qualitatively model a simple shear. In some cases, this profile can be seen as describing a transient response to an imposed gradient in the presence of turbulent diffusion.

We consider the vertical profiles of longitudinal velocity $u(z)$, density $\rho(z)$ and dynamic viscosity $\mu(z)$ given by the relations:

$$\begin{aligned} u(z) &= U_1 F\left(\lambda, \frac{z-h}{\delta_u}\right), \\ \rho(z) &= (\rho_0 - \rho_1) F\left(\lambda, \frac{z-h}{\delta_\rho}\right) + \rho_1, \quad \mu(z) = (\mu_0 - \mu_1) F\left(\lambda, \frac{z-h}{\delta_\mu}\right) + \mu_1, \end{aligned} \quad (3)$$

where δ_u , δ_ρ and δ_μ are the thicknesses respectively associated to the profiles $u(z)$, $\rho(z)$ and $\mu(z)$. We consider here the case where these three thicknesses are equal to $\delta=0.3 \text{ m}$. The boundaries of the simulation field are defined by equations $z=0$ and $z=3h$, the height $z=h=1 \text{ m}$ being the interface location. In addition, we have chosen $\lambda=0.1$, since diffusion is assumed to be greater in water than in mud flow. The corresponding profiles are presented in figure 2.

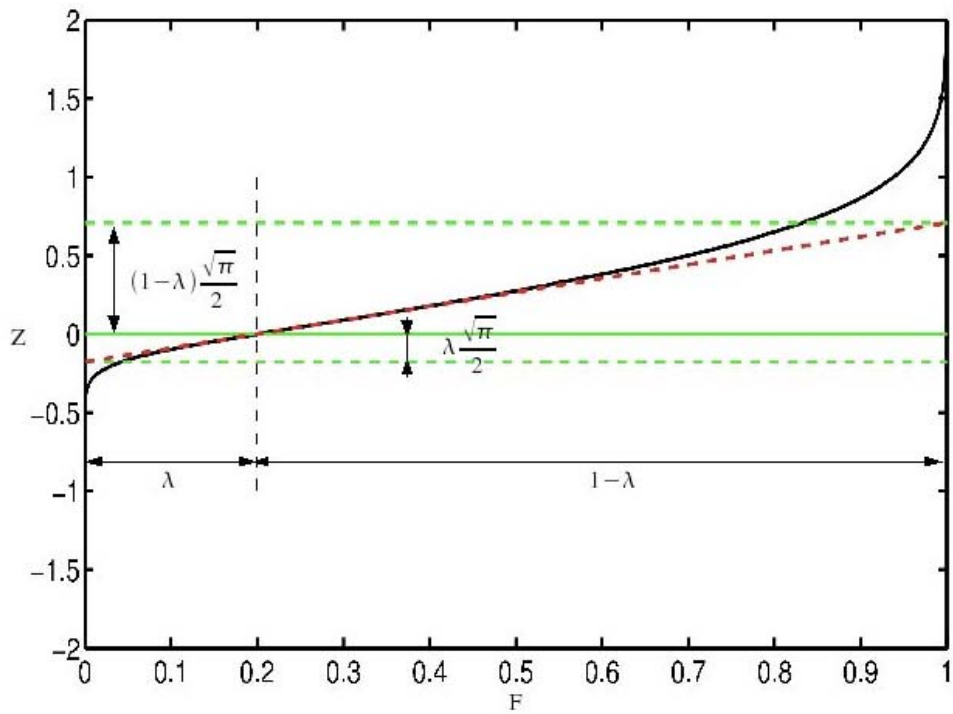


Figure 1. Representation of profile on Z of the function $F(\lambda, Z)$ with $\lambda=0.2$.

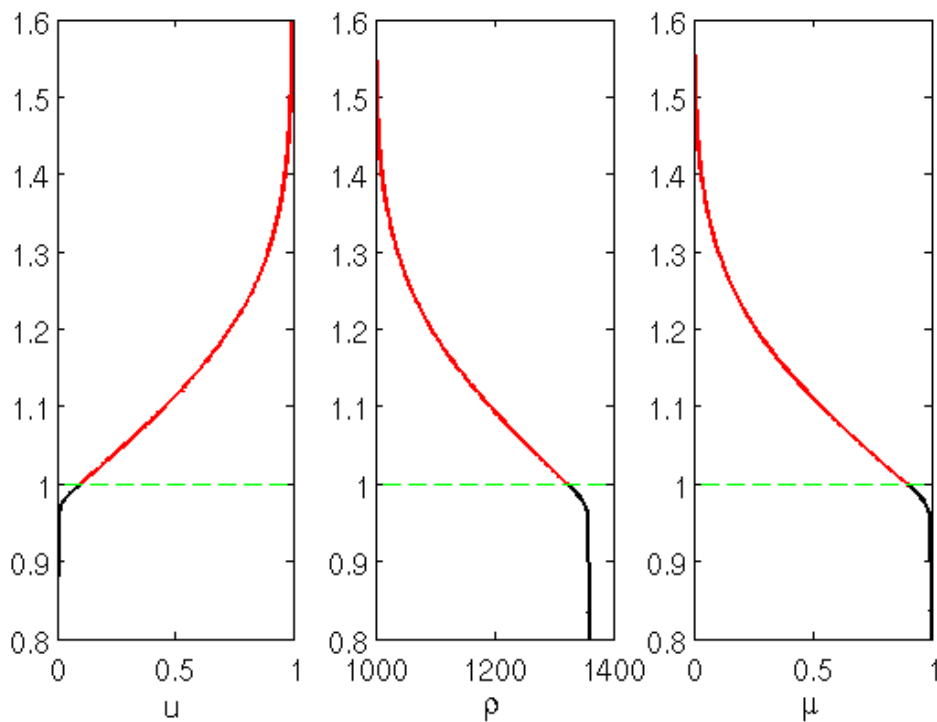


Figure 2. Initial profiles $u(z)$, $\rho(z)$ and $\mu(z)$ on a portion $z \in [0.8 \text{ m}, 1.6 \text{ m}]$ of the domain $z \in [0, 3 \text{ h}]$, with $h=1 \text{ m}$, $\delta=0.3 \text{ m}$ and $\lambda=0.1$.

2.3 Control parameters

First, in the chosen configurations, the Atwood number $At = (\rho_1 - \rho_0) / (\rho_1 + \rho_0)$ is close to 0.15. The three other non-dimensional numbers, relevant for our study, are defined by:

$$Re = \frac{U_0 \delta}{\mu_0 / \rho_0}, \quad Ri = \frac{g (\rho_0 - \rho_1) \delta \sqrt{\pi}}{\rho_h 2U_0^2} \quad \text{and} \quad W = \log_{10} \left(\frac{\mu_1}{\mu_0} \right), \quad (4)$$

where $\rho_h = \rho(h) = (\rho_0 - \rho_1) \lambda + \rho_1$ is the density at the interface, Re is the Reynolds number based on the viscosity of water, Ri is the Richardson number Ri based on the maximum of the density gradient located at the interface $z=h$, and W is the logarithm of the viscosity ratio between mud flow and water.

2.4 Description of the Navier-Stokes and linear stability analysis code

The Navier-Stokes solver, JADIM, developed at IMFT (Institut de Mécanique des Fluides de Toulouse), solves Navier-Stokes equations for multiphase incompressible flows. The equations use primitive variables (velocity, pressure) and are solved by a finite volumes method. The code is 2nd order accurate in space and time, thanks to a 3rd order Runge-Kutta temporal scheme and a semi-implicit Crank-Nicolson scheme for diffusive terms. The equations are discretized using a 2nd order centered scheme with staggered variables (CALMET & MAGNAUDET 1996, LEGENDRE & MAGNAUDET 1998). The version used in the present study solves the system of equations (1) and has been validated for a viscosity gradient by ERN *et al.*, 2003 and for a density gradient by HALLEZ, 2007.

As supplement to the JADIM code, a linear stability code, LiSa (ANTKOWIAK & BRANCHER 2004, 2007) is used to obtain a global vision of the problem. This code solves the system of equations (1) linearized around the base flow (3). Given a parallel base flow, a perturbation (defined by its wave vector) and specific numerical parameters, LiSa provides the eigen values and their associated modes, using a spectral method based on Chebyshev polynomials. So, in 2D, for each wave length, LiSa gives the prediction of the more unstable mode and its growth rate.

3. Results

For the simulations, the density of water and mud flow are fixed, while we vary the characteristic velocity U_0 to modify the Richardson number Ri and the Reynolds number Re , and the density of the mud flow to modify the parameter W . For these simulations, the Reynolds number order is 10^5 .

3.1 Bidimensionnal parameters

First, two-dimensional simulations, similar to flows observed in estuaries, are carried out with the JADIM code. The choice of a 2D configuration has been justified by an exploration of 3D configurations, in which we observed the development of instabilities

in the flow direction. However, instabilities with a finite spanwise wave number cannot be excluded by the Squire Theorem, as done for homogeneous flows.

The 2D simulations are performed on a periodic field streamwise, of 3.4 m length and 3 m height, with respectively 340×300 grid points, and with no slip boundary condition at the bottom and free-slip condition at the top. At initial time, the parallel flow is perturbed by a vertical velocity field located around the interface $z=h$ modeled by a white noise of amplitude $w_m=10^{-2} \text{ m s}^{-1}$.

3.2 Typical growth of instabilities

We present here results of 2D simulations, realized with the JADIM code, by varying the Richardson gradient number Ri and the viscosity ratio W . We observe the appearance of growing shear instabilities of large amplitude for Richardson numbers below the critical Richardson number of 0.25, approximately, for all the values of W investigated here.

As for the viscosity gradient, we observe that, as presented in figures 3 and 4 for a Richardson number $Ri=0.15$, an increase of the viscosity gradient leads to a shift of the instability location upward in the interface, that is, closer to water, the less viscous fluid. This shift of the instability leads to a reducing of the quantity of sediments put in suspension. Indeed, for a large viscosity ratio, mixing occurs between clear water and some already mixed mud, of intermediate density and viscosity.

3.3 Linear stability analysis

After having determined the impact of control parameters on the stability of the interface, linear stability analysis has been performed using the LiSa code developed at IMFT. The growth rate of the more unstable mode is computed for a hundred values of the normalized wavenumber of the perturbation k^* and is presented in figure 6 for $Ri=0.15$ and different W . We choose to scale the wave number with half the thickness of the interface: $k^*=k \times \delta \times (\sqrt{\pi})/4$; the phase velocity with $U_0/2$; the growth rate is normalized by $\sigma^*=\sigma \times (\delta \times (\sqrt{\pi})/2) / U_0$.

We observe, in figure 5, a similar behavior for the different viscosity ratios tested here. However, slight differences are observed for $W=3$, corresponding to a dynamic viscosity of mud flow 1000 times higher than that of water. On the one hand, we notice that the growth rate is larger ($\sim 10\%$); and on the other hand, the most unstable wave number is different (0.456 for $W=0$ and 0.480 for $W=3$).

This difference in growth rate and wave number of the most unstable modes between different W , can be of consequence for the sediment resuspension.

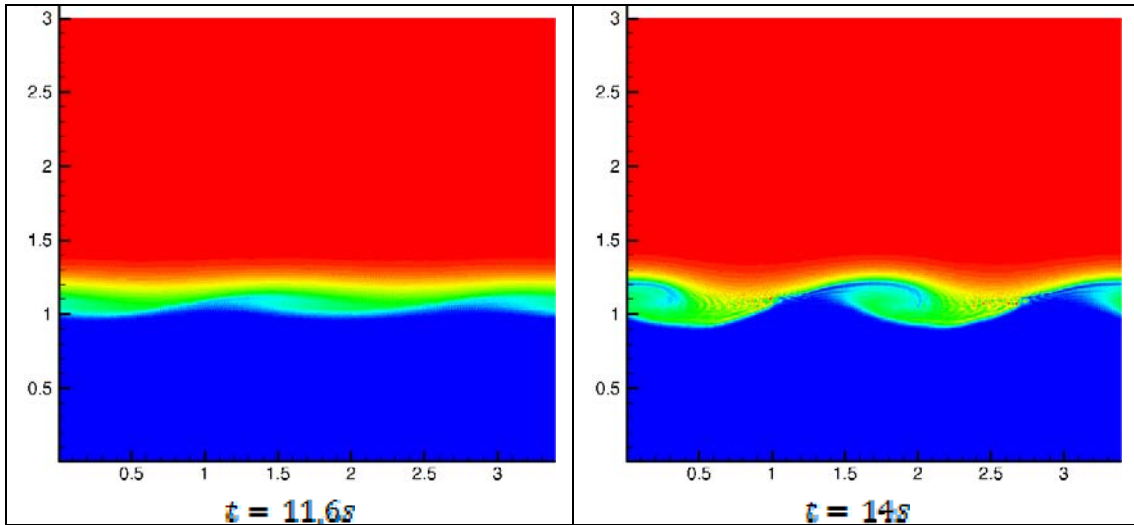


Figure 3. Configuration $Ri=0.15$, $L=3.4$ m, $W=0$. Density fields $\rho(x, z)$ at different times separated by 2.3 s ($\color{red}\blacksquare$: $\rho_0=1000$ kg m⁻³, $\color{blue}\blacksquare$: $\rho_1=1360$ kg m⁻³).

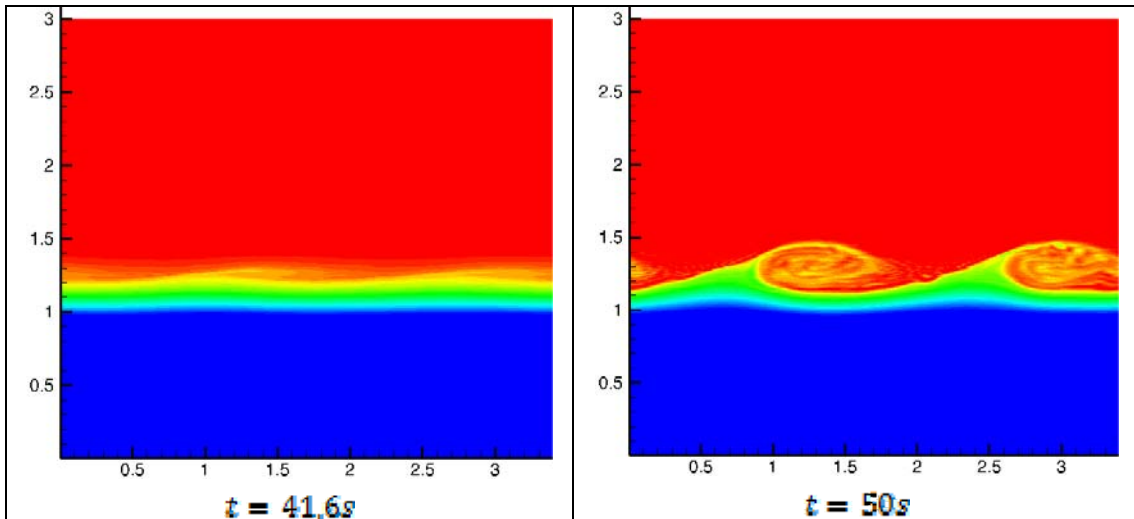


Figure 4. Configuration $Ri=0.15$, $L=3.4$ m, $W=3$. Density fields $\rho(x, z)$ at different times separated by 8.4 s ($\color{red}\blacksquare$: $\rho_0=1000$ kg m⁻³, $\color{blue}\blacksquare$: $\rho_1=1360$ kg m⁻³).

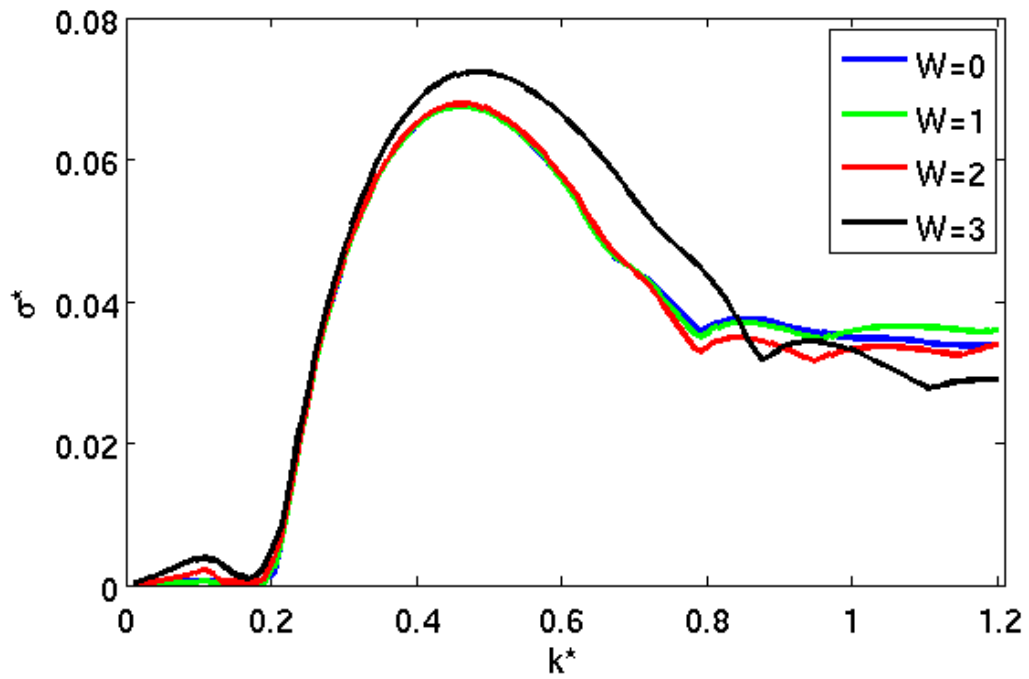


Figure 5 : Representation of the normalized growth rate σ^* as a function of the normalized wave number k^* for Richardson number $Ri=0.15$.

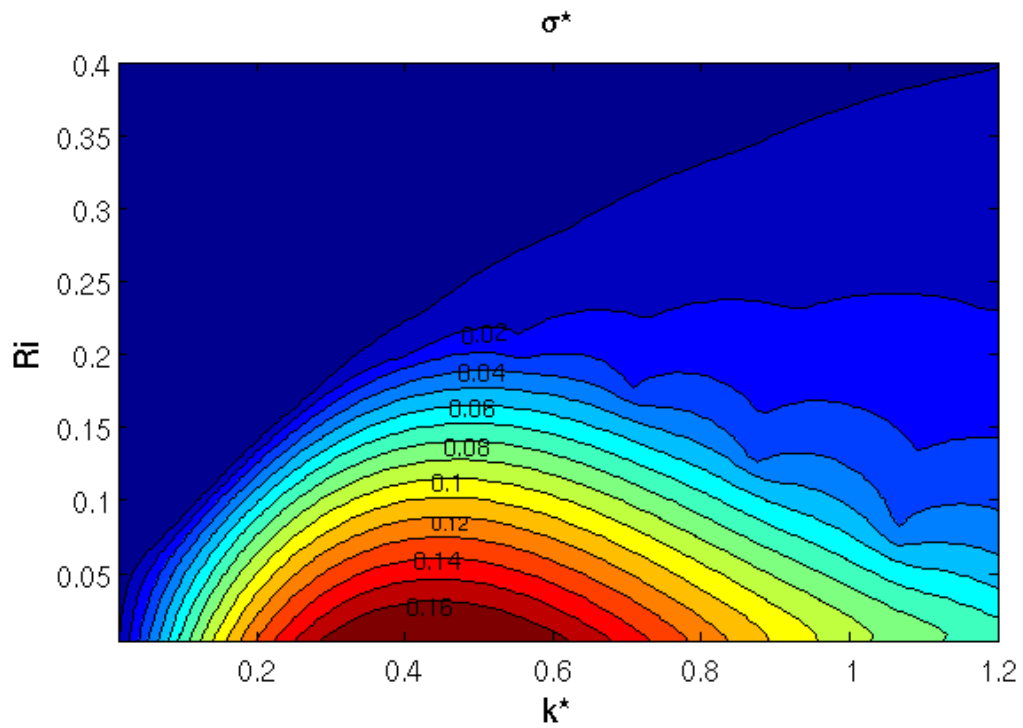


Figure 6 : Isolines of the normalized growth rate σ^* , as a function of the non-dimensional wave number k^* and the Richardson number Ri (for $W=3$).

In figure 6, we clearly observe, when Ri decreases, an increase of the growth rate and a decrease of the most unstable wave number. We can also observe for this configuration ($W=3$) the subsistence of very small growth rate instabilities beyond the conventional critical Richardson number situated at 0.25.

4. Conclusion

We have modeled the interface between water and mud flow by two Newtonian miscible fluids presenting strong variations of density and viscosity. 2D flows are simulated to get a stability criterion which is observed to be close to the well-known theoretical value $Ri=1/4$ for density stratified shear flows of homogeneous viscosity. The results show that the viscosity gradient modifies the outbreak of the instability, thus modifying the critical Richardson number, the wave number of the most unstable mode and the location of the instability at the interface. Therefore the viscosity ratio needs to be taken into account for the parameterization of the mixing due to shear instabilities. These results predict, at the interface, the density of a homogeneous fluid, resulting from the mixing of a model of mudflow and water, in function of flow feature. The next goal is to translate the density in concentration to supply a boundary condition of sediment resuspension. These results suggest also further investigations, for instance, by comparing the present analysis to simulations realized with a more realistic rheology of the mud flow like Bingham or complex rheology (PHAM VAN BANG, 2007).

5. Acknowledgements



The first author is supported by a scholarship intended for PhD students funded by the DGA (Direction Générale de l'Armement).

This work has benefited from CICT and GENCI computational means.

6. Bibliography

- ANTKOWIAK A., BRANCHER P. (2004). *Transient energy growth for the Lamb-Oseen vortex*. Physics of Fluids, vol. 16(1), pp L1-L4. doi:10.1063/1.1626123
- ANTKOWIAK A., BRANCHER P. (2007). *On vortex rings around vortices: an optimal mechanism*. Journal of Fluids Mechanics, vol. 578, pp 295-304. doi:10.1017/S0022112007005198
- CALMET I., MAGNAUDET J. (1996). *Large-eddy simulation of high-Schmidt number mass transfer in a turbulent channel flow*. Physics of Fluids, vol. 9(2), pp 438-455. doi:10.1063/1.869138
- CAULFIELD C.P., PELTIER W.R. (2000). *The anatomy of the mixing transition in homogeneous and stratified free shear layers*. Journal of Fluid Mechanics, n° 413, pp 1-47. doi:10.1017/S0022112000008284

- DEARDORFF J.W., WILLIS G.E. (1982). *Dependence of mixed-layer entrainment on shear stress and velocity jump*. Journal of Fluid Mechanics, n° 115, pp 123–150. doi:10.1017/S0022112082000688
- ERN P., CHARRU F., LUCHINI P. (2003). *Stability analysis of a shear flow with strongly stratified viscosity*. Journal of Fluid Mechanics, n° 496, pp 295–312. doi:10.1017/S0022112003006372
- HALLEZ Y. (2007). *Mélange gravitationnel de fluides en géométrie confinée*. Thèse, Institut National Polytechnique de Toulouse, 140 p. Available online URL <http://oa.imft.fr/1851/1/hallez2007.pdf>
- HOGG A.McC., IVEY G.N. (2003). *The Kelvin-Helmoltz to Holmboe instability transition in stratified exchange flows*. Journal of Fluid Mechanics, vol. 477, pp 339-362. doi:10.1017/S0022112002003397
- KRANENBURG C., WINTERWERP J.C. (1997). *Erosion of fluid mud layers. I: Entrainment model*. Journal of Hydraulic Engineering, vol. 123, n° 6, pp 504-511. doi:10.1061/(ASCE)0733-9429(1997)123:6(504)
- LEGENDRE D. (1996). *Quelques aspects des forces hydrodynamiques et des transferts de chaleur sur une bulle sphérique*. Thèse, Institut National Polytechnique de Toulouse, 266 p. Available online URL <http://ethesis.inp-toulouse.fr/archive/00000655/>
- LE NORMAND C. (1995). *Modélisation numérique tridimensionnelle des processus de transport des sédiments cohésifs en environnement estuarien*. Thèse, Institut National Polytechnique de Toulouse, 237 p.
- MEHTA A.J., HAYTER E.J., PARKER W.R., KRONE R.B., TEETER A.M. (1989). *Cohesive sediments transport*. Journal of Hydraulic Engineering, vol. 115, n° 8, pp 1076-1112. doi:10.1061/(ASCE)0733-9429(1989)115:8(1076)
- PARCHURE T.M., MEHTA A.J. (1985). *Erosion of soft cohesive sediment deposits*. Journal of Hydraulic Engineering, vol. 111(10), pp 1308-1326. doi:10.1061/(ASCE)0733-9429(1985)111:10(1308)
- PARTHENIADES E. (1965). *Erosion and deposition of cohesive soils*. Journal of Hydraulic Division, ASCE, vol. 91(1), pp 105-137.
- PHAM VANG BANG D., OVARLEZ G., TOCQUER L. (2007). *Effets de la densité et de la structuration sur les caractéristiques rhéologiques de la vase*. La Houille Blanche, pp 85-93. doi:10.1051/lhb:2007023

Appendix : Notations

A_0	: quantity A associated with the water
A_1	: quantity A associated with mud flow
A^*	: normalized quantity A
At	: Atwood number
F	: function
g	: acceleration of gravity (m s^{-2})
h	: height of the interface water - mud flow (m)
k	: streamwise wave number
L	: length of the computational box (m)
P	: pressure (Pa)
Re	: Reynolds number
Ri	: Richardson gradient number
t	: time (s)
\underline{u}	: velocity vector (m s^{-1})
w_m	: amplitude of the vertical velocity perturbations (m s^{-1})
W	: logarithm of the viscosity ratio
x,y,z	: coordinates (m)
Z	: vertical coordinate associated with function F (here $Z=(z-h)/\delta$)
δ	: thickness of interface (m)
λ	: shape ratio between water and mud flow
μ	: dynamic viscosity (Pa s)
ρ	: density (kg m^{-3})
σ	: growth rate
Φ	: volume fraction of mud flow in fluid

